

Two Tungstates Containing Platinum Nanoparticles Prepared by Air-Calcining Keggin-Type Polyoxotungstate-Coordinated Diplatinum(II) Complexes: Effect on Sintering-Resistance and Photocatalysis

メタデータ	言語: en 出版者: Springer Nature 公開日: 2021-11-26 キーワード (Ja): キーワード (En): 作成者: Kato, Chika Nozaki, Kubota, Toshiya, Aono, Koki, Ozawa, Naoto メールアドレス: 所属:
URL	http://hdl.handle.net/10297/00028429



Two Tungstates Containing Platinum Nanoparticles Prepared by Air-Calcining Keggin-Type Polyoxotungstate-Coordinated Diplatinum(II) Complexes: Effect on Sintering-Resistance and Photocatalysis

Chika Nozaki Kato^{1,2} · Toshiya Kubota¹ · Koki Aono¹ · Naoto Ozawa¹

Received: 14 September 2021 / Accepted: 25 October 2021
© The Author(s) 2021

Abstract

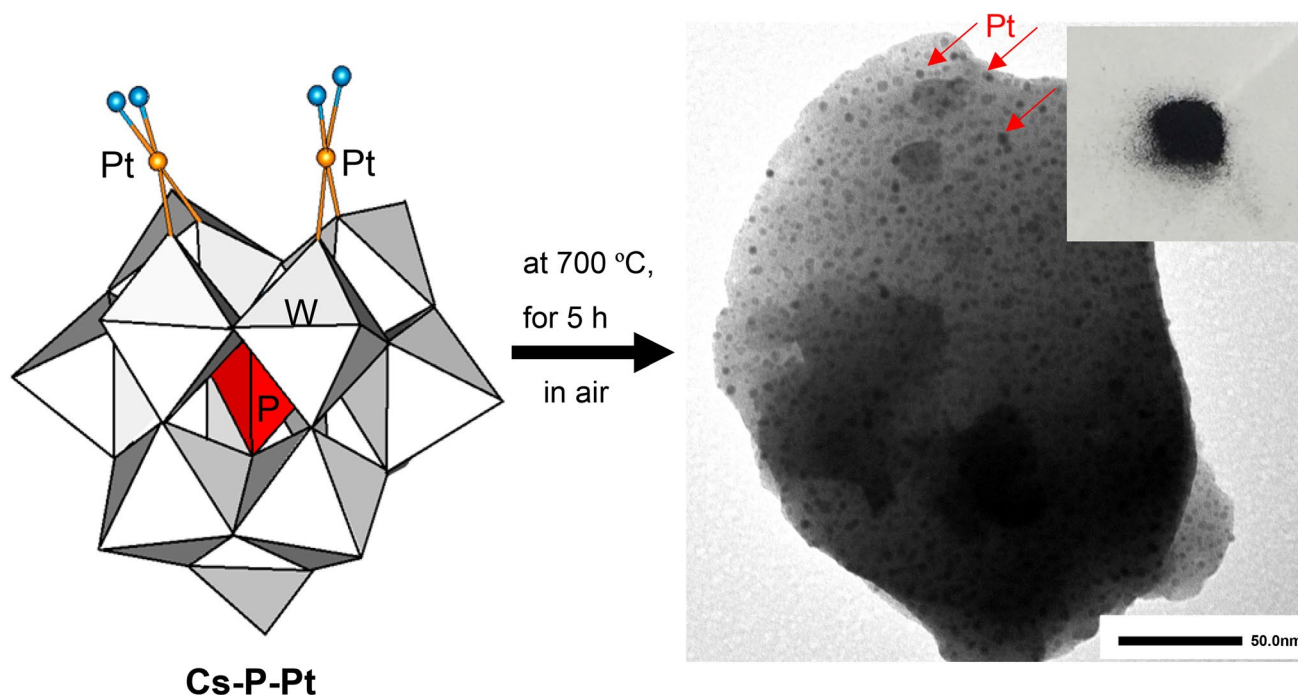
Two tungstates containing platinum nanoparticles (Pt Npts) were obtained by air-calcining α -Keggin-type diplatinum(II)-coordinated polyoxotungstates, $\text{Cs}_3[\alpha\text{-PW}_{11}\text{O}_{39}\{\text{cis-Pt}(\text{NH}_3)_2\}_2] \cdot 8\text{H}_2\text{O}$ (**Cs-P-Pt**) and $\text{Cs}_4[\alpha\text{-SiW}_{11}\text{O}_{39}\{\text{cis-Pt}(\text{NH}_3)_2\}_2] \cdot 11\text{H}_2\text{O}$ (**Cs-Si-Pt**), at 700–900 °C for 5 h. The polyoxotungstate **Cs-P-Pt** was transformed to a mixture of Pt Npts and $\text{Cs}_3\text{PW}_{12}\text{O}_{40}$ upon calcination, while the **Cs-Si-Pt** structures were transformed to Pt Npts and $\text{Cs}_4\text{W}_{11}\text{O}_{35}$. The Pt Npts generated by air-calcining **Cs-P-Pt** at 700 °C for 5 h were uniform with an average particle size of 3.6 ± 1.1 nm, which was much smaller than that of the Pt Npts obtained by calcining **Cs-Si-Pt** (19.9 ± 9.9 nm) under identical conditions. This demonstrated the significant inhibitory effect of **Cs-P-Pt** on aggregation during high-temperature air-calcination at a high platinum content (10.6 wt.%) and in the absence of a support. During calcination at 700–900 °C, **Cs-P-Pt** exhibited higher activities than **Cs-Si-Pt** with respect to hydrogen evolution from aqueous triethanolamine solutions under visible light irradiation in the presence of Eosin Y, α -Keggin-type mono-aluminum-substituted polyoxotungstate, and titanium dioxide. When **Cs-P-Pt** was calcined at 800 °C for 100 h, no decrease in activity was observed in comparison with that upon calcination for 5 h.

✉ Chika Nozaki Kato
kato.chika@shizuoka.ac.jp

¹ Department of Chemistry, Faculty of Science, Shizuoka University, 836 Ohya, Suruga-ku, Shizuoka 422-8529, Japan

² Research Institute of Green Science and Technology, Shizuoka University, 836 Ohya, Suruga-ku, Shizuoka 422-8529, Japan

Graphical Abstract



Keywords Polyoxometalate · Platinum nanoparticle · Photocatalysts · Calcination · Hydrogen evolution

1 Introduction

Platinum nanoparticle catalysts are extensively used in various industrial processes, including hydrogenation, naphtha reforming, oxidation, automotive exhaust catalysis, and fuel generation (fuel cells) [1, 2]. However, supported platinum nanoparticle catalysts frequently agglomerate into large particles at high reaction temperatures, losing their catalytically active surface areas [3]. For the suppression of such thermally induced deactivation, complex nanostructures, including core-shell nanostructures [4] and well-designed pore structures [5] have been proposed. Although these methods have been successful in maintaining the platinum nanostructures, aggregation still occurs at higher platinum contents and under thermal treatment at higher temperatures.

For the preparation of supported platinum catalysts, various platinum compounds, such as H_2PtCl_6 , $\text{Pt}(\text{NH}_3)_4\text{Cl}_2$, $\text{Pt}(\text{NH}_3)_4(\text{OH})_2$, $\text{Pt}(\text{NH}_3)_4(\text{NO}_3)_2$, $\text{H}_2\text{Pt}(\text{OH})_6$, and $\text{Pt}(\text{C}_5\text{H}_7\text{O}_2)_2$ are used as precursors [2]. These compounds are heat-treated in the presence of various gases (air, oxygen, hydrogen, H_2O , N_2 , and Ar) or under vacuum. In each case, the ligand was eliminated during the heat treatment, and reduction of the oxidized platinum sites (Pt^{2+} and Pt^{4+}) to Pt^0 was observed. Further high-temperature treatment induced aggregation.

Lacunary polyoxometalates (POMs) can be used as inorganic ligands to form various types of complexes via coordination of metal ions and organometallics to the vacant site(s) [6–9]. Several structurally well-defined Pt^{2+} -containing POMs, such as $[\text{Pt}_2(\text{W}_5\text{O}_{18})_2]^{8-}$ [10], $[\textit{anti}\text{-Pt}_2(\alpha\text{-PW}_{11}\text{O}_{39})_2]^{10-}$ [11], and $[\textit{syn}\text{-Pt}_2(\alpha\text{-PW}_{11}\text{O}_{39})_2]^{10-}$ [11] have been reported. Recently, we have synthesized cesium and tetramethylammonium salts of α -Keggin and α_2 -Dawson diplatinum(II)-coordinated polyoxotungstates, including $\text{Cs}_3[\alpha\text{-PW}_{11}\text{O}_{39}\{\textit{cis}\text{-Pt}(\text{NH}_3)_2\}_2] \cdot 8\text{H}_2\text{O}$, $[(\text{CH}_3)_4\text{N}]_3[\alpha\text{-PW}_{11}\text{O}_{39}\{\textit{cis}\text{-Pt}(\text{NH}_3)_2\}_2] \cdot 10\text{H}_2\text{O}$, $[(\text{CH}_3)_4\text{N}]_4[\alpha\text{-SiW}_{11}\text{O}_{39}\{\textit{cis}\text{-Pt}(\text{NH}_3)_2\}_2] \cdot 13\text{H}_2\text{O}$, $[(\text{CH}_3)_4\text{N}]_4[\alpha\text{-GeW}_{11}\text{O}_{39}\{\textit{cis}\text{-Pt}(\text{NH}_3)_2\}_2] \cdot 11\text{H}_2\text{O}$, $[(\text{CH}_3)_4\text{N}]_4\text{H}[\alpha\text{-AlW}_{11}\text{O}_{39}\{\textit{cis}\text{-Pt}(\text{NH}_3)_2\}_2] \cdot 11\text{H}_2\text{O}$, $[(\text{CH}_3)_4\text{N}]_4\text{H}[\alpha\text{-BW}_{11}\text{O}_{39}\{\textit{cis}\text{-Pt}(\text{NH}_3)_2\}_2] \cdot 9\text{H}_2\text{O}$, $\text{Cs}_4[\alpha\text{-GeW}_{11}\text{O}_{39}\{\text{Pt}(\text{bpy})\}_2] \cdot 10\text{H}_2\text{O}$ (bpy = 2,2'-bipyridine), $\text{Cs}_{3.5}\text{H}_{0.5}[\alpha\text{-GeW}_{11}\text{O}_{39}\{\text{Pt}(\text{phen})\}_2] \cdot 3\text{H}_2\text{O}$ (phen = 1,10-phenanthroline), and $\text{Cs}_6[\alpha_2\text{-P}_2\text{W}_{17}\text{O}_{61}\{\textit{cis}\text{-Pt}(\text{NH}_3)_2\}_2] \cdot 13\text{H}_2\text{O}$ using a similar approach, and demonstrated a long-term steady production of hydrogen with highly effective utilization of the platinum centers for hydrogen production from aqueous ethylenediaminetetraacetic acid disodium salt ($\text{EDTA} \cdot 2\text{Na}$) and triethanolamine (TEOA) solutions under visible light irradiation [12–16].

In the process of improving the activities of the platinum sites, it was found that air calcination of a cesium salt of α -Keggin diplatinum(II)-coordinated silicotungstate, $\text{Cs}_4[\alpha\text{-SiW}_{11}\text{O}_{39}\{\text{cis-Pt}^{\text{II}}(\text{NH}_3)_2\}_2]\cdot 11\text{H}_2\text{O}$, at low temperatures (e.g., 300 °C) led to a hydrophilic colloidal species, $\text{Cs}_4[\{\text{Pt}(\text{OH})_2\}_2\cdot\text{SiW}_{12}\text{O}_{40}]$ that exhibited excellent photocatalytic activities toward hydrogen evolution from aqueous TEOA solutions under visible-light irradiation [17].

In this paper, we report the formation of two types of tungstates containing Pt Npts, via air-calcination of $\text{Cs}_3[\alpha\text{-PW}_{11}\text{O}_{39}\{\text{cis-Pt}(\text{NH}_3)_2\}_2]\cdot 8\text{H}_2\text{O}$ (**Cs-P-Pt**) and $\text{Cs}_4[\alpha\text{-SiW}_{11}\text{O}_{39}\{\text{cis-Pt}^{\text{II}}(\text{NH}_3)_2\}_2]\cdot 11\text{H}_2\text{O}$ (**Cs-Si-Pt**) at temperatures ranging from 700 °C to 900 °C. The -Keggin-type polyoxotungstate unit that remained after calcination had a significant role in suppressing the aggregation of the platinum nanostructures. The calcined samples were characterized using thermogravimetric/differential thermal analysis (TG/DTA), Fourier transform infrared (FT-IR) spectroscopy, X-ray photoelectron spectroscopy (XPS), powder X-ray diffraction (PXRD), and transmission electron microscopy (TEM). The photocatalytic activities of the calcined samples toward hydrogen production from aqueous TEOA solutions were also investigated in the presence of Eosin Y (EY), Keggin-type mono-aluminum-coordinated polyoxometalate, $\text{K}_5[\alpha\text{-SiW}_{11}\{\text{Al}(\text{OH}_2)\}\text{O}_{39}]\cdot 7\text{H}_2\text{O}$, and titanium dioxide under visible light irradiation ($\lambda \geq 440$ nm).

2 Experimental

2.1 Materials and Reagents

$\text{Cs}_3[\alpha\text{-PW}_{11}\text{O}_{39}\{\text{cis-Pt}(\text{NH}_3)_2\}_2]\cdot 8\text{H}_2\text{O}$ (**Cs-P-Pt**) [13], $\text{Cs}_4[\alpha\text{-SiW}_{11}\text{O}_{39}\{\text{cis-Pt}(\text{NH}_3)_2\}_2]\cdot 11\text{H}_2\text{O}$ (**Cs-Si-Pt**) [17], $[(\text{CH}_3)_4\text{N}]_3[\alpha\text{-PW}_{11}\text{O}_{39}\{\text{cis-Pt}(\text{NH}_3)_2\}_2]\cdot 10\text{H}_2\text{O}$ (**TMA-P-Pt**) [12], $[\text{Pt}(\text{NH}_3)_4]_2[\alpha\text{-SiW}_{12}\text{O}_{40}]\cdot 4\text{H}_2\text{O}$ (**Pt-SiW12**) [17], $\text{Na}_3[\alpha\text{-PW}_{12}\text{O}_{40}]\cdot 10\text{H}_2\text{O}$ [18], $\text{K}_4[\alpha\text{-SiW}_{12}\text{O}_{40}]\cdot 17\text{H}_2\text{O}$ [19], $\text{K}_8[\alpha\text{-SiW}_{11}\text{O}_{39}]\cdot 17\text{H}_2\text{O}$ [20], and $\text{Cs}_4\text{W}_{11}\text{O}_{35}$ [21] were prepared via methods described in the literature. The numbers of solvated water molecules were determined through TG/DTA measurements. All reagents and solvents were obtained from commercial sources and used as received. Titanium dioxide (anatase:rutile = 80:20) and platinum black (≤ 20 μm ; $\geq 99.95\%$ purity) were obtained from Wako Pure Chemical Industries, Ltd. and Sigma-Aldrich Co. LLC., respectively.

2.2 Instrumentation and Analytical Procedures

The infrared spectra were recorded on a PerkinElmer Spectrum100 FT-IR spectrometer in KBr discs at approximately 25 °C in air. The services of Eurofins EAG Materials Science (USA) were enlisted for performing XPS analyses. A

monochromated Al K_α radiation (1486.6 eV) was used as the X-ray source. The binding energies are referenced to the C_{1s} binding energy at 284.8 eV. Powder X-ray diffraction (PXRD) measurements were performed on an X-ray powder diffractometer (SmartLab, Rigaku, Corp., Japan) using Cu K_α radiation ($K\alpha = 1.54$ Å). Transmission electron microscopy (TEM) images were recorded using a JEOL-JEM 2100F electron microscope, and the elemental compositions of the samples were studied using energy-dispersive X-ray spectroscopy (EDS, JED-2300 T (JEOL, Japan)).

2.3 Photocatalytic Reaction Experiments

Typical photocatalytic reactions were performed at 25 °C. EY and $\text{K}_5[\alpha\text{-SiW}_{11}\{\text{Al}(\text{OH}_2)\}\text{O}_{39}]\cdot 7\text{H}_2\text{O}$ (2.5 μmol) were dissolved in 10 mL of 100 mM aqueous TEOA solution at pH 7.0. Subsequently, the calcined samples (containing 0.2 μmol Pt) and titanium dioxide (anatase:rutile = 80:20; 50 mg) were suspended in this solution. The suspension was placed in a glass reaction vessel, which was connected to a Pyrex conventional closed gas circulation system (245.5 cm^3). The photoreaction was initiated by light irradiation using a 300 W Xe lamp equipped with a cut-off filter ($\lambda \geq 440$ nm). The evolution of hydrogen, oxygen, carbon monoxide, and methane was analyzed using a gas chromatography (GC) instrument equipped with a thermal conductivity detector (TCD), 5 Å molecular sieves, and stainless-steel columns. The samples were assigned after comparison with standard samples analyzed under identical conditions. The turnover number (TON) was calculated as $2[\text{H}_2 \text{ evolved (mol)}]/[\text{Pt atoms (mol)}]$.

3 Results and Discussion

When **Cs-P-Pt** was calcined at temperatures from 25 °C to 800 °C at a heating rate of 40 °C min^{-1} , followed by maintaining at 800 °C for 5 h in air (without flow), its color changed from yellow to black (the calcined sample was denoted as **Cs-P-Pt-800-5**), and the obtained powder was insoluble in water.

The FT-IR spectrum of **Cs-P-Pt-800-5** contains several bands at 1079 cm^{-1} , 985 cm^{-1} , 888 cm^{-1} , and 804 cm^{-1} , as shown in Fig. 1a. These bands are remarkably different from those of as-prepared **Cs-P-Pt** (1099 cm^{-1} , 1047 cm^{-1} , 955 cm^{-1} , 915 cm^{-1} , 859 cm^{-1} , 801 cm^{-1} , 757 cm^{-1} , and 721 cm^{-1}) (Fig. 1b) [13] but almost identical to those of $\text{Na}_3[\alpha\text{-PW}_{12}\text{O}_{40}]\cdot 12\text{H}_2\text{O}$ (1080 cm^{-1} , 984 cm^{-1} , 893 cm^{-1} , and 808 cm^{-1}) [18] and $\text{Cs}_3[\alpha\text{-PW}_{12}\text{O}_{40}]$ (1080 cm^{-1} , 890 cm^{-1} , and 798 cm^{-1}) [22], suggesting that the structure of the α -Keggin-type mono-lacunary polyoxotungstate ligand, $\{\text{PW}_{11}\text{O}_{39}\}$, in **Cs-P-Pt** transformed to $\{\text{PW}_{12}\text{O}_{40}\}$ under the applied thermal treatment conditions. The band

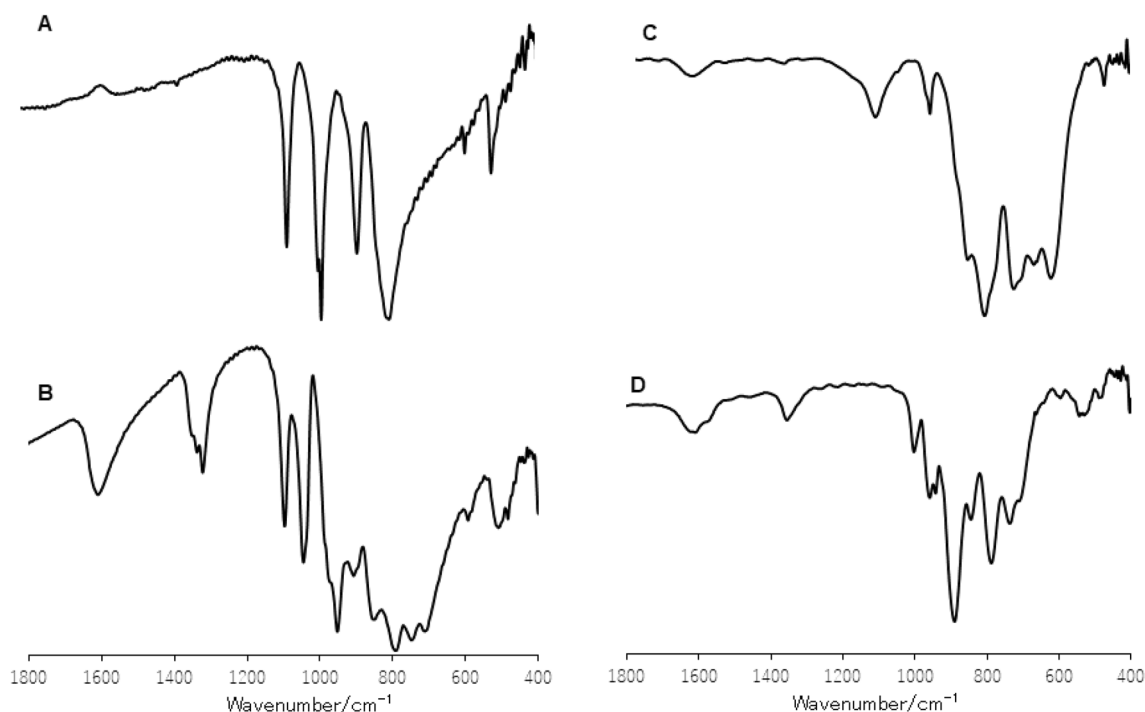


Fig. 1 FT-IR spectra of **a** Cs-P-Pt-800-5, **b** Cs-P-Pt, **c** Cs-Si-Pt-800-5, and **d** Cs-Si-Pt

at 1356 cm^{-1} corresponding to the four NH_3 groups disappeared, indicating the complete removal of the four ammonia molecules. The same bands as **Cs-P-Pt-800-5** were observed for the samples obtained by calcination at $700\text{ }^\circ\text{C}$ and $900\text{ }^\circ\text{C}$ (these samples are denoted as **Cs-P-Pt-700-5** and **Cs-P-Pt-900-5**, respectively), as shown in Fig. S1. This proved that the α -Keggin structure was maintained at least up to $900\text{ }^\circ\text{C}$.

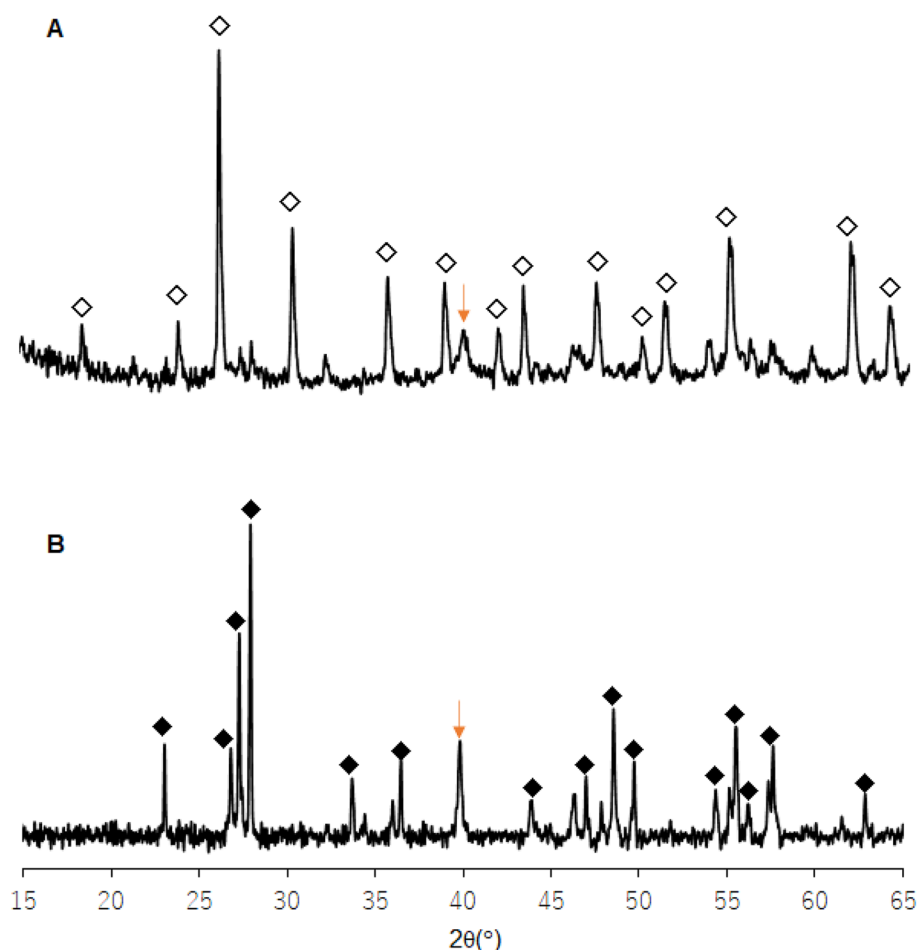
When **Cs-Si-Pt** was calcined at $800\text{ }^\circ\text{C}$ for 5 h (the calcined sample is denoted as **Cs-Si-Pt-800-5**), its color changed from yellow to gray, and the obtained powder was insoluble in water. The FT-IR spectrum (Fig. 1c) of **Cs-Si-Pt-800-5** showed bands at 968 cm^{-1} , 889 cm^{-1} , 861 cm^{-1} , 812 cm^{-1} , 779 cm^{-1} , 730 cm^{-1} , 717 cm^{-1} , and 672 cm^{-1} , which were different from those observed for the as-prepared **Cs-Si-Pt** (1004 cm^{-1} , 960 cm^{-1} , 944 cm^{-1} , 891 cm^{-1} , 846 cm^{-1} , 789 cm^{-1} , 738 cm^{-1} , and 712 cm^{-1}) (Fig. 1d) but similar to those of $\text{Cs}_4\text{W}_{11}\text{O}_{35}$ (969 cm^{-1} , 860 cm^{-1} , 816 cm^{-1} , 780 cm^{-1} , 707 cm^{-1} , and 675 cm^{-1}), which was obtained via a method described in the literature [21]. The same spectral pattern (Fig. S2) was observed when **Cs-Si-Pt** was calcined at $700\text{ }^\circ\text{C}$ and $900\text{ }^\circ\text{C}$ (the calcined samples are denoted as **Cs-Si-Pt-700-5** and **Cs-Si-Pt-900-5**). The four NH_3 groups coordinated to the di-platinum site in **Cs-Si-Pt** were vaporized, as previously reported [17]. A band appeared at 1123 cm^{-1} which was attributed to the Si-O-Si stretching, suggesting that the internal $\{\text{SiO}_4\}$ unit in the Keggin structure was transformed to silicon oxide [23].

The PXRD pattern of **Cs-P-Pt-800-5** (Fig. 2a) showed the same peaks as that of $\text{Cs}_3\text{PW}_{12}\text{O}_{40}$ (ICDD: 00-050-1857), and similar peaks were observed for **Cs-P-Pt-700-5** and **Cs-P-Pt-900-5**, as shown in Fig. S3. These results prove that the $\{\text{PW}_{11}\text{O}_{39}\}$ unit in **Cs-P-Pt** was transformed to $\{\text{PW}_{12}\text{O}_{40}\}$ under the reported thermal treatment conditions. This was validated by the FT-IR spectra. In contrast, the PXRD pattern of **Cs-Si-Pt-800-5** (Fig. 2b) exhibited the same peaks as that of $\text{Cs}_4\text{W}_{11}\text{O}_{35}$ (ICDD: 00-051-1891). A similar structural transformation of the $\{\text{SiW}_{11}\text{O}_{39}\}$ unit to $\{\text{W}_{11}\text{O}_{35}\}$ was observed for **Cs-Si-Pt-700-5** and **Cs-Si-Pt-900-5**, as shown in Fig. S4. As previously reported, the $\{\text{SiW}_{11}\text{O}_{39}\}$ unit in **Cs-Si-Pt** was transformed to $\{\text{SiW}_{12}\text{O}_{40}\}$ by air calcination in the lower temperature range of $250\text{--}500\text{ }^\circ\text{C}$ [17]. However, at higher temperatures in the range of $700\text{ }^\circ\text{C}$ to $900\text{ }^\circ\text{C}$, the Keggin structure was transformed to $\{\text{W}_{11}\text{O}_{35}\}$.

A broad peak corresponding to Pt(111) ($2\theta(^{\circ}) = 40$, ICDD: 00-04-0802) was observed. This indicates that the di-platinum(II) sites in **Cs-P-Pt** and **Cs-Si-Pt** were reduced to crystalline Pt(0) by the applied thermal treatment. As shown in Figs. 2, S3 and S4, the peak intensity increased as the calcination temperature was increased. These results suggest that the crystallite size of platinum increases with the calcination temperature.

The Pt(4f) XPS spectra of **Cs-P-Pt-800-5** and **Cs-Si-Pt-800-5** are shown in Fig. 3. In both the spectra, the platinum sites were primarily composed of Pt^0 , with low levels of Pt^{2+} and Pt^{4+} . The occurrence of Pt^{4+} needs to be

Fig. 2 Powder XRD patterns of **a Cs-P-Pt-800-5** and **b Cs-Si-Pt-800-5**. The peaks of $\text{Cs}_3\text{PW}_{12}\text{O}_{40}$, $\text{Cs}_4\text{W}_{11}\text{O}_{35}$, and Pt(111) are marked with white and black rhombuses, and a red arrow, respectively



interpreted with caution because of the high levels of signal overlap with Cs(4d). The W(4f) XPS spectra (Figs. S5a and S6a) of **Cs-P-Pt-800-5** and **Cs-Si-Pt-800-5** showed that the tungsten sites were composed of W^{6+} . The Cs(3d) XPS spectra of **Cs-P-Pt-800-5** and **Cs-Si-Pt-800-5** indicated that the existence of cesium in the monovalent form, as shown in Figs. S5b and S6b.

Figure 4a and b show TEM images of **Cs-P-Pt-700-5** and **-800-5**. The corresponding size distributions are shown in Figs. 4c and 4d. Homogeneously dispersed Pt Npts can be observed as small black grains in the tungstate matrix. The average sizes of the Pt Npts in the calcined samples are summarized in Table 1. Surprisingly, **Cs-P-Pt-700-5** and **Cs-P-Pt-800-5** exhibited average particle sizes of 3.6 ± 1.1 nm and 5.3 ± 2 nm, respectively, at a high platinum content (10.6 wt.%), in the absence of a support. The average particle size of **Cs-P-Pt-900-5** was 9.3 ± 2.8 nm, which was approximately twice that of **Cs-P-Pt-800-5**, indicating slight aggregation at 900 °C (Fig. S7). However, the average particle size reached upon calcination at 800 °C for 100 h was 5.4 ± 1.9 nm, and negligible aggregation of Pt Npts was observed after long-term heat treatment, as shown in Fig. S8.

In contrast, the average sizes of the Pt Npts in **Cs-Si-Pt-700-5**, **-800-5**, and **-900-5** were 19.9 ± 9.9 nm, 42.8 ± 21.2 nm, and 100.8 ± 70.7 nm, respectively, and the particle sizes increased remarkably with the calcination temperature, as shown in Figs. 5, S9a, and S10. The black grains were confirmed to be platinum particles via tungsten and platinum EDS mapping (Figs. S9b and 9c).

As a control experiment, Pt Npt-supported TiO_2 (Pt content: 11 wt.%) was prepared as follows: *cis*-diamminedichloroplatinum(II) (cisplatin) (0.169 g; 0.56 mmol) was dissolved in 50 mL water. TiO_2 (0.83 g) was added to the solution, and the mixture was stirred for 2 h at approximately 25 °C. After evaporation to dryness at 100 °C, the obtained solid was calcined at 700 °C for 5 h in air. The calcined product was denoted as **cisplatin/TiO₂-700-5**. The average particle size of **cisplatin/TiO₂-700-5** was 31.4 ± 19.7 nm, which was larger than that of **Cs-P-Pt-700-5** and **Cs-Si-Pt-700-5**, as shown in Fig. S11. When the platinum salt of α -Keggin silicotungstate $[\text{Pt}(\text{NH}_3)_4]_2[\alpha\text{-SiW}_{12}\text{O}_{40}] \cdot 4\text{H}_2\text{O}$ (platinum content: 11.2 wt.%) was calcined at 800 °C for 5 h in air (the calcined product was denoted as **Pt-SiW12-800-5**), particles with non-uniform sizes were formed with some particles growing above 50 nm

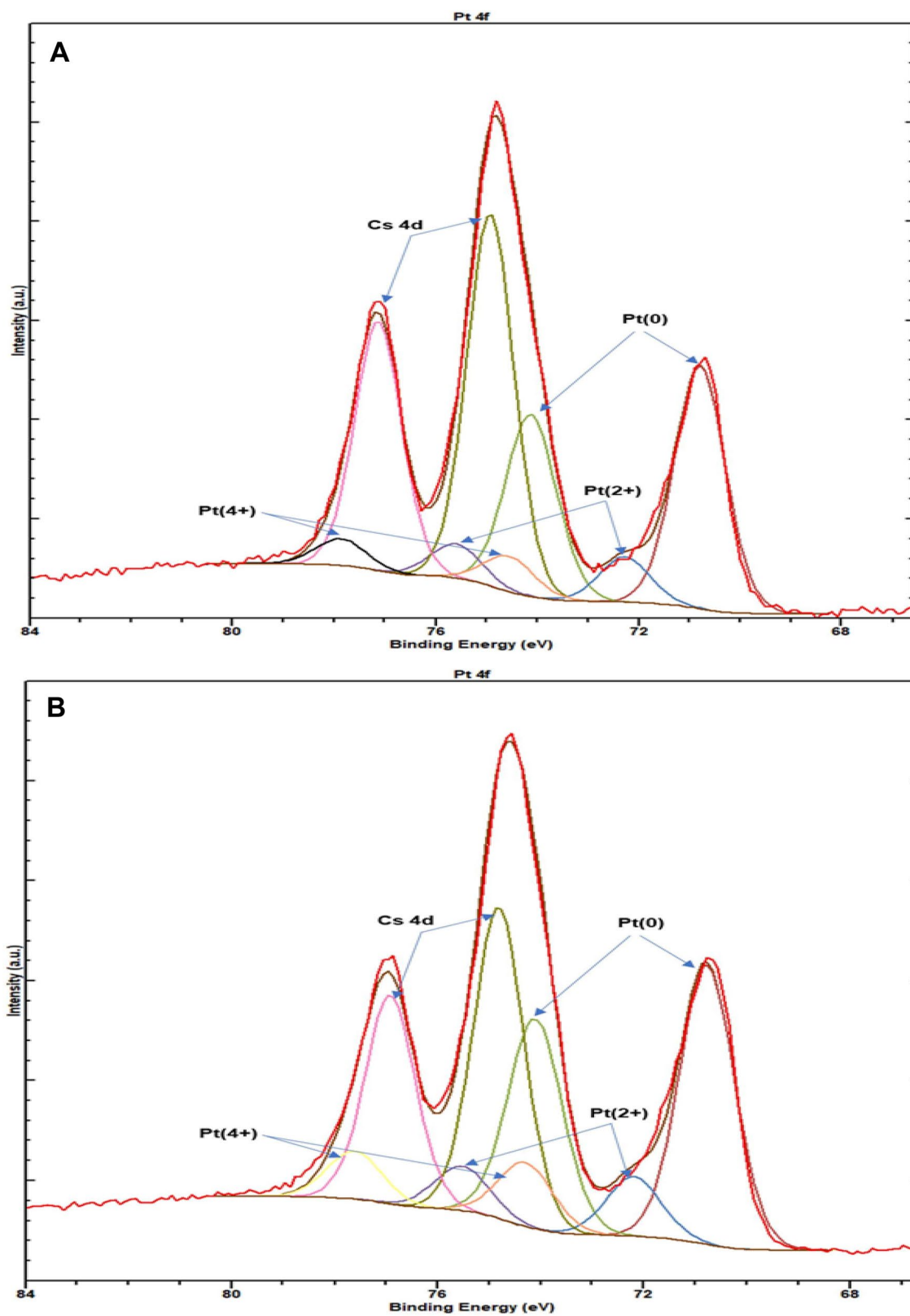


Fig. 3 Pt(4f) XPS spectra in the range 66.5–84 eV of **a** Cs-P-Pt-800-5 and **b** Cs-Si-Pt-800-5

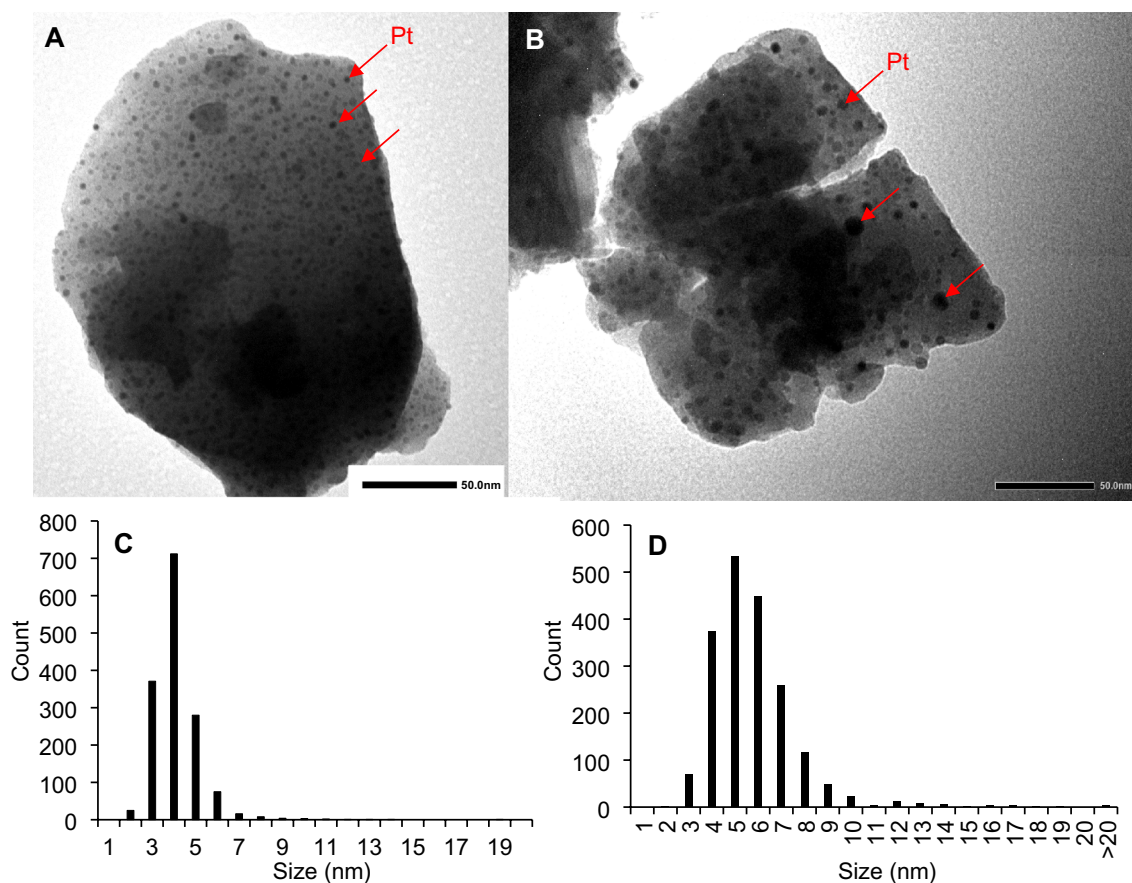


Fig. 4 TEM images of **a** Cs-P-Pt-700-5 and **b** Cs-P-Pt-800-5. The Pt particle size distributions of Pt Npts in Cs-P-Pt-700-5 and Cs-P-Pt-800-5 are shown in **c** and **d**, respectively

Table 1 Average size of Pt Npts in the calcined samples

calcined sample	Pt content (wt.%)	average Pt Npts size (nm)
Cs-P-Pt-700-5	10.6 ^a	3.6 ± 1.1
Cs-P-Pt-800-5		5.3 ± 2
Cs-P-Pt-900-5		9.3 ± 2.8
Cs-P-Pt-800-100		5.4 ± 1.9
Cs-Si-Pt-700-5	10.1 ^a	19.9 ± 9.9
Cs-Si-Pt-800-5		42.8 ± 21.2
Cs-Si-Pt-900-5		100.8 ± 70.7
cisplatin/TiO ₂ -700-5	11.0	31.4 ± 19.7

^aThe platinum contents were calculated based on the composition formulae of Cs-P-Pt and Cs-Si-Pt

(Fig. S12a). It can be seen from the FT-IR spectrum of Pt-SiW₁₂-800-5 (Fig. S12b) that the Keggin-type structure was decomposed and {W₁₁O₃₅} unit was not formed. A platinum salt of phosphotungstate retaining the structure of PW₁₂O₄₀³⁻ could not be obtained using the same method as that used to obtain SiW₁₂O₄₀⁴⁻. It was confirmed from

the FT-IR spectrum (Fig. S13b) that the Keggin structure was decomposed when TMA-P-Pt (platinum content: 11 wt.%) was calcined at 800 °C for 5 h in air (the obtained sample was denoted as TMA-P-Pt-800-5). The particle size was non-uniform, and some particles grew to several tens of nanometers, as shown in Fig. S13a.

According to these results, Cs-P-Pt, which retained the α -Keggin polyoxotungstate and Cs₃PW₁₂O₄₀ after calcination, exhibited an excellent aggregation inhibitory effect at high platinum content and in the absence of a support. Such inhibition of platinum aggregation is not observed in platinum compounds from which the ligands disappear upon calcination [2]. It is critical to coordinate the platinum species to the mono-vacant sites in α -Keggin-type mono-lacunary phosphotungstates and isolate them as cesium salts for the expression of such an effect.

The activities of the Pt Npts in the calcined samples as co-catalysts were studied by using Cs-P-Pt-800-5 and Cs-Si-Pt-800-5 to catalyze the evolution of hydrogen from aqueous TEOA solutions under light irradiation ($\lambda \geq 440$ nm) in the presence of Eosin Y (EY), K₅[α -SiW₁₁{Al(OH₂)O₃₉}]·7H₂O (denoted as K-Si-Al), and titanium dioxide

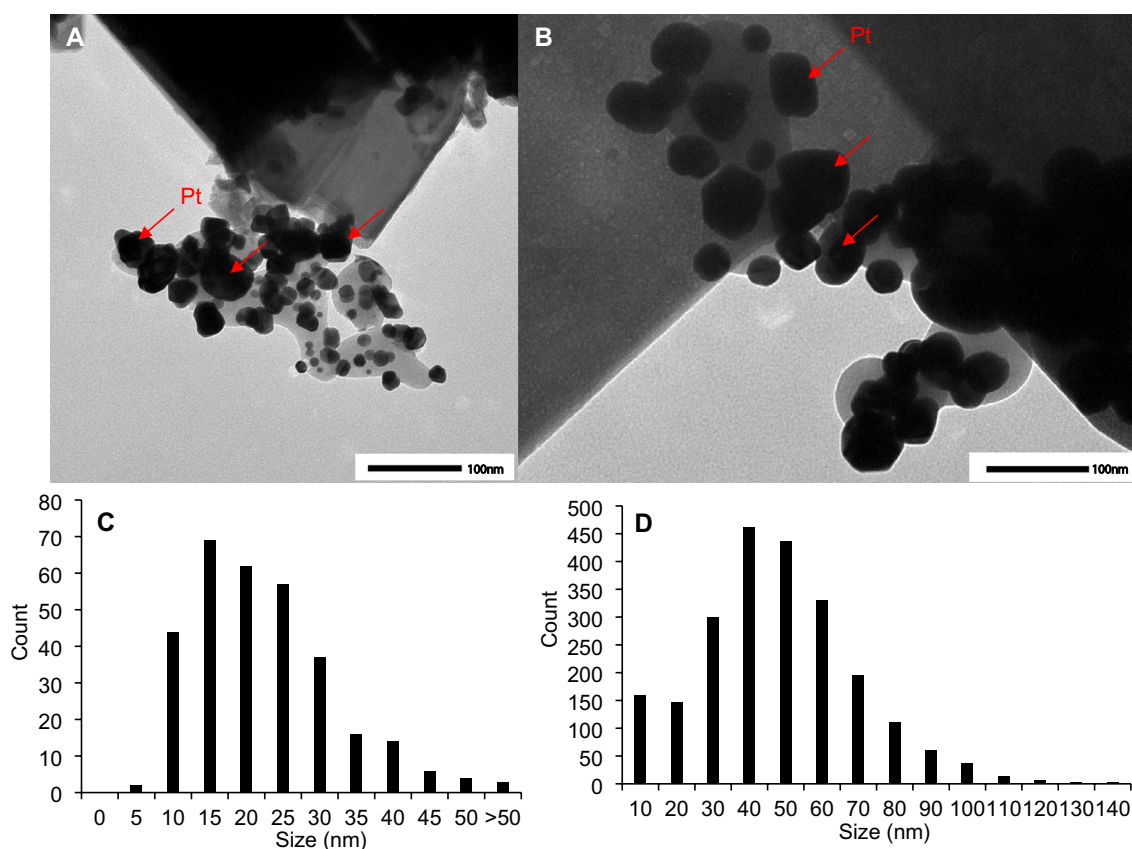


Fig. 5 TEM images of **a** Cs-Si-Pt-700-5 and **b** Cs-Si-Pt-800-5. The Pt particle size distributions in Cs-Si-Pt-700-5 and Cs-Si-Pt-800-5 are shown in **c** and **d**, respectively

(anatase:rutile = 80:20), as shown in Figs. 6a and b [14, 17, 24, 25]. The precursors, Cs-P-Pt and Cs-Si-Pt were weighted while ensuring that the amount of platinum was 0.2 μmol (the contents of Pt in the catalysts containing TiO_2 and the platinum samples were 0.084 wt.% and 0.080 wt.%, respectively). Subsequently, they were calcined at 800 $^\circ\text{C}$ for 5 h in air. TEOA was used as the sacrificial reagent. EY and K-Si-Al were used as the photosensitizer and EY stabilizer, respectively. Although TiO_2 was used to promote charge separation, the tungstates containing Pt Npts were not supported on the surface of TiO_2 . In order to compare the activities with the samples before calcination, TiO_2 was simply dispersed in the solutions. Hydrogen was formed with 100% selectivity, and oxygen, carbon dioxide, carbon monoxide, and methane were not detected under these reaction conditions. It has already been confirmed that no reaction was observed in the absence of platinum catalysts or Eosin Y under the reported conditions.

After 6 h of light irradiation, the amounts of hydrogen evolved in presence of Cs-P-Pt-800-5 and Cs-Si-Pt-800-5 were 180 μmol and 156 μmol , respectively. The TONs ($=2[\text{hydrogen evolved (mol)}]/[\text{Pt atoms (mol)}]$) observed for Cs-P-Pt-800-5 and Cs-Si-Pt-800-5 were 1801 and

1556, respectively. These values were higher than those of Cs-P-Pt and Cs-Si-Pt (TONs observed after 6 h were 703 and 409, respectively). These results suggest that the photocatalytic activities of Cs-P-Pt and Cs-Si-Pt were improved upon calcination. The turnover frequencies (TOF = TON/reaction time (h)) of Cs-P-Pt-800-5 and Cs-Si-Pt-800-5 after 1 h were 685 and 336 h^{-1} , respectively. These values are higher than those of similar photocatalytic systems containing platinum co-catalysts prepared via the photo-reduction of H_2PtCl_6 , EY, and TiO_2 . For example, the TOFs of Pt/EY/nitrogen-doped TiO_2 [26], Pt/EY/modified TiO_2 with phosphate [27], Pt/EY/ $\text{Fe}^{3+}/\text{TiO}_2$ [28], and Pt/EY/ $\text{SiW}_{11}\text{O}_{39}^{8-}/\text{TiO}_2$ [25] are less than 150 h^{-1} with respect to hydrogen evolution from aqueous TEOA solutions under visible-light irradiation. When platinum black (3.0 μmol Pt) was used as a co-catalyst, the TOF after 1 h was 11.7 h^{-1} , which was significantly lower than those of Cs-P-Pt-800-5 and Cs-Si-Pt-800-5. It is difficult to discuss the differences in activities based on the sizes of the Pt Npts alone because of the influences of $\text{Cs}_3\text{PW}_{12}\text{O}_{40}$ and $\text{Cs}_4\text{W}_{11}\text{O}_{35}$ contained in Cs-P-Pt-800-5 and Cs-Si-Pt-800-5, respectively. However, upon calcination at 700–900 $^\circ\text{C}$, Cs-P-Pt showed higher activities than Cs-Si-Pt, as shown in Fig. 7. Upon

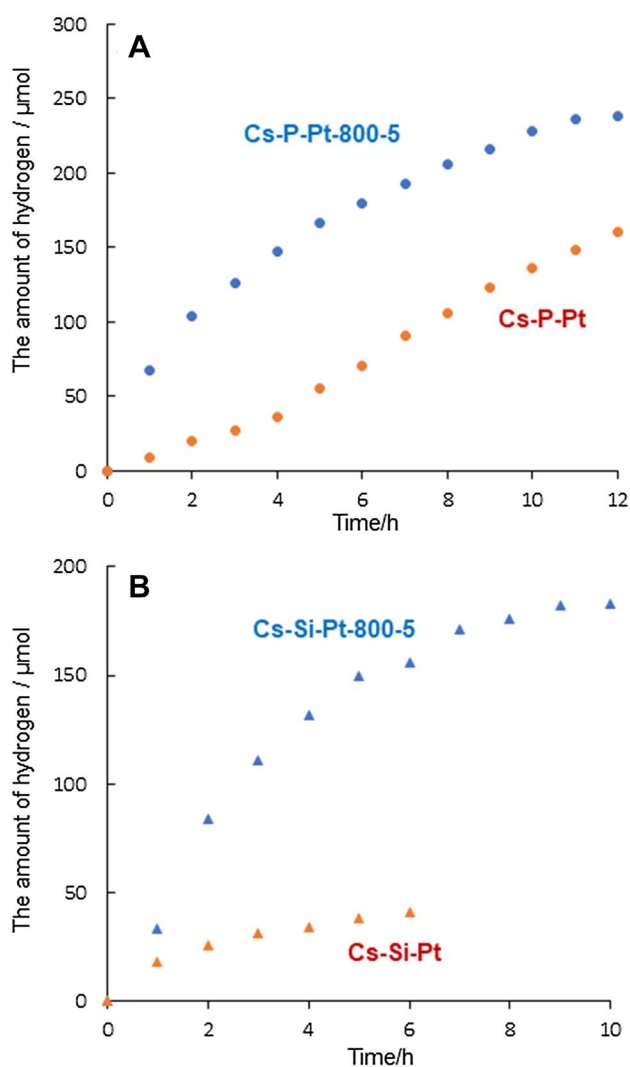


Fig. 6 Time course for hydrogen evolution catalyzed by **a Cs-P-Pt-800-5** and **Cs-P-Pt**, and **b Cs-Si-Pt-800-5** and **Cs-Si-Pt**. Reaction conditions: platinum catalyst (0.2 μmol Pt), EY (2.5 μmol), **K-Si-Al** (2.5 μmol), TiO_2 (anatase:rutile=80:20) 50 mg, 100 mM aqueous TEOA solution (10 mL, pH 7), light irradiation ($\lambda \geq 440$ nm), 25 $^\circ\text{C}$

using **Cs-P-Pt-800-100**, 192 μmol hydrogen was generated after 6 h (TON: 1919), and there was no reduction in catalytic activity upon extending the calcination time from 5 h to 100 h.

In the cases of **Cs-P-Pt-800-5** and **Cs-Si-Pt-800-5**, the amount of hydrogen generated gradually decreased with time, as shown in Figs. 6a and b. For the hydrophilic platinum-polyoxotungstate colloidal particles obtained by air-calcining **Cs-Si-Pt** at 300 $^\circ\text{C}$ for 5 h, the TON after 3 h exceeded 4600 under similar reaction conditions. However, rapid decomposition of the platinum sites was observed and the activity did not improve upon re-addition of EY [17]. To confirm that **Cs-P-Pt-800-5** was not decomposed, we performed the following experiment: The

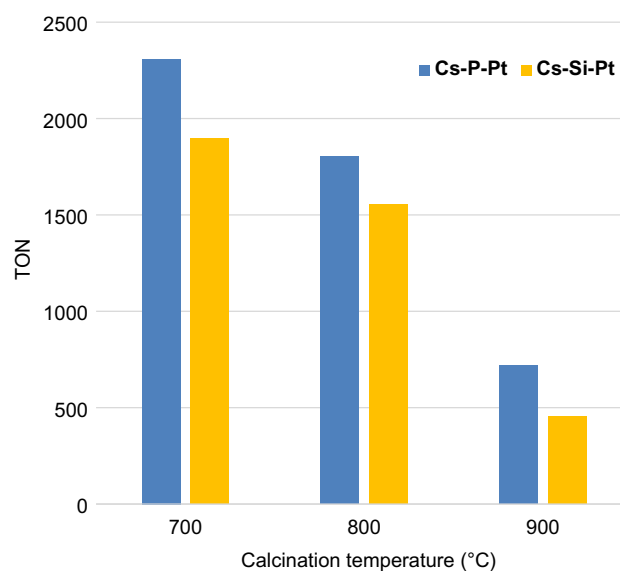


Fig. 7 A plot of TON after 6 h vs. calcination temperature of **Cs-P-Pt** and **Cs-Si-Pt** for hydrogen evolution from aqueous TEOA under visible light irradiation. Reaction conditions are shown in the caption of Fig. 6

aforementioned photocatalytic reaction was performed in the presence of **Cs-P-Pt-800-5** (0.2 μmol Pt) under light irradiation for 20 h. The residual solid was collected using a membrane filter (JG 0.2 μm) and washed with water and ethanol. Thereafter, the solid containing **Cs-P-Pt-800-5** and TiO_2 was dispersed again in an aqueous TEOA solution containing EY and **K-Si-Al**. After 6 h of light irradiation, approximately 200 μmol of hydrogen was generated. It was also confirmed that the photocatalytic activity of **Cs-Si-Pt-800-5** was restored by the re-addition of EY (Fig. S14). These results demonstrate that **Cs-P-Pt-800-5** and **Cs-Si-Pt-800-5** did not decompose under the applied reaction conditions and were recyclable.

Finally, the following experiment was conducted to investigate the sizes of the Pt Npts after light irradiation: **Cs-P-Pt-800-5** (37.6 mg) was dispersed in aqueous TEOA containing dissolved EY, and subjected to light irradiation for 6 h. The residual solid was collected through a membrane filter (JG 0.2 μm) and washed with water and ethanol. The TEM images and the corresponding size distributions of the obtained samples are shown in Figs. 8a and b. After light irradiation, homogeneously dispersed Pt Npts were observed in the tungstate matrix. The average particle size was 5.1 ± 2.5 nm, which was nearly the same as that prior to light irradiation. Although it has been reported that the sizes of Pt Npts increase during hydrogen evolution under light irradiation [29], no aggregation of the Pt Npts comprising **Cs-P-Pt-800-5** was observed under the applied reaction conditions.

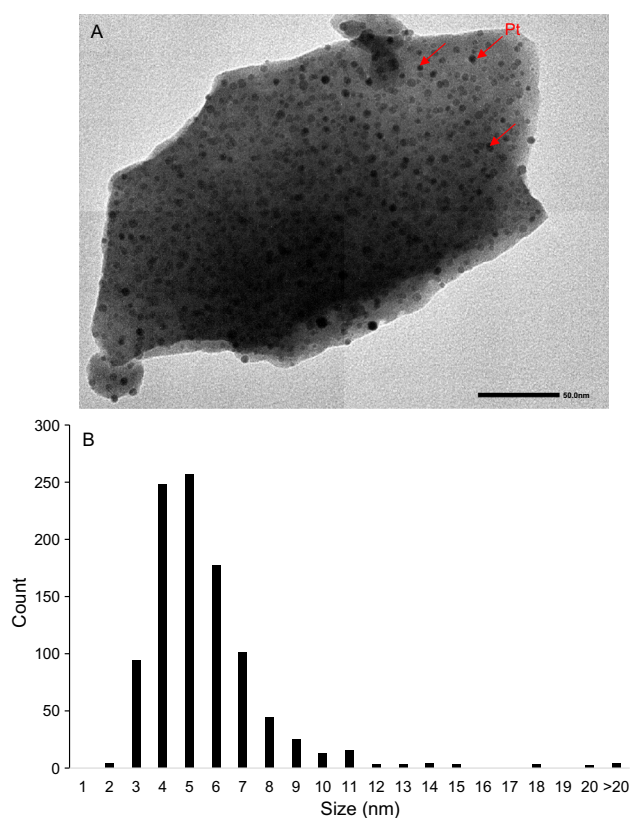


Fig. 8 a TEM image of **Cs-P-Pt-800-5** after light irradiation, and **b** the size distribution of Pt Npts

This reaction mechanism is similar to that of a reported Pt co-catalyst/EY/K-Al-Si/TiO₂ system [14]. However, since the water-insoluble calcined samples were used without being supported on the surface of titanium oxide, it is possible that the efficiency of electron transfer between titanium oxide and the platinum and/or tungstate sites was reduced. Sintering at high temperatures may also induce three-dimensional microstructural changes and inhibit proton transfer to the platinum sites. In order to overcome these problems, we are investigating methods to support the calcined samples on the surfaces of some semiconducting photocatalytic materials. The results will be reported in due course.

4 Conclusion

Two tungstates containing platinum nanoparticles were obtained by air-calcining Cs₃[α-PW₁₁O₃₉{*cis*-Pt(NH₃)₂]₂·8H₂O (**Cs-P-Pt**) and Cs₄[α-SiW₁₁O₃₉{*cis*-Pt(NH₃)₂]₂·11H₂O (**Cs-Si-Pt**), at 700–900 °C for 5 h. When **Cs-P-Pt** was calcined, its {PW₁₁O₃₉} unit transformed to {PW₁₂O₄₀}. In contrast, **Cs-Si-Pt** exhibited a structural transformation of the {SiW₁₁O₃₉} unit to {W₁₁O₃₅} under identical calcination

conditions. The di-platinum(II) sites in **Cs-P-Pt** and **Cs-Si-Pt** transformed to Pt Npts. The average particle size of Pt Npts generated via air-calcination of **Cs-P-Pt** was much smaller than that observed when **Cs-Si-Pt** was calcined. Thus, **Cs-P-Pt** exhibited an excellent aggregation inhibitory effect at high platinum content and in the absence of a support.

The calcined samples were applied as co-catalysts for hydrogen evolution from aqueous TEOA solutions under visible light irradiation ($\lambda \geq 440$ nm) in the presence of Eosin Y, K₅[α-SiW₁₁{Al(OH₂)}O₃₉]·7H₂O, and titanium dioxide. Upon calcination at 700–900 °C, **Cs-P-Pt** exhibited higher activities than **Cs-Si-Pt**. The activity of **Cs-P-Pt** did not diminish after calcination at 800 °C for 100 h, in comparison with its activity after 5 h of calcination. It was also confirmed that the **Cs-P-Pt** sample calcined at 800 °C for 5 h exhibited no change in the sizes of the Pt Npts when subjected to light irradiation. Platinum aggregation was thus suppressed under the applied photocatalytic reaction conditions.

Supplementary Information The online version contains supplementary material available at <https://doi.org/10.1007/s10562-021-03843-x>.

Acknowledgements This work was supported by JSPS KAKENHI Grant Number JP19H02489, and the Research Institute of Green Science and Technology Fund for Research Project Support (2021-RIGST-21E03) at National University Corporation, Shizuoka University. We acknowledge Mr. Ryota Kasai (Shizuoka University) for supporting several experiments on the photocatalytic reactions.

Declarations

Conflict of interest The authors of this work declare that a potential competing interest does not exist. There is not any financial or personal interest or belief that could affect this research work.

Open Access This article is licensed under a Creative Commons Attribution 4.0 International License, which permits use, sharing, adaptation, distribution and reproduction in any medium or format, as long as you give appropriate credit to the original author(s) and the source, provide a link to the Creative Commons licence, and indicate if changes were made. The images or other third party material in this article are included in the article's Creative Commons licence, unless indicated otherwise in a credit line to the material. If material is not included in the article's Creative Commons licence and your intended use is not permitted by statutory regulation or exceeds the permitted use, you will need to obtain permission directly from the copyright holder. To view a copy of this licence, visit <http://creativecommons.org/licenses/by/4.0/>.

References

1. R.J.Farrauto and C.H.Bartholomew, Fundamentals of Industrial Catalytic Processes (Blackie Academic & Professional, 1997)
2. Radivojević D, Seshan K, Lefferts L (2006) Preparation of well-dispersed Pt/SiO₂ catalysts using low-temperature treatments. Appl Catal A: Gen 301:51–58

- Yati I, Ridwan M, Jeong GE, Lee Y, Choi J, Yoon CW, Suh DJ, Ha J (2014) Effects of sintering-resistance and large metal-support interface of alumina nanorod-stabilized Pt nanoparticle catalysts on the improved high temperature water gas shift reaction activity. *Catal Commun* 56:11–16
- Liu B, Xu H, Zhang Z (2012) Platinum based core-shell catalysts for sour water-gas shift reaction. *Catal Commun* 26:159–163
- De Rogatis L, Cargnello M, Gombac V, Lorenzuti B, Montini T, Fornasiero P (2010) Embedded phases: a way to active and stable catalysts. *ChemSuschem* 3:24–42
- M.T. Pope, *Heteropoly and isopoly oxometalates* (Springer, 1983)
- Pope MT, Müller A (1991) Chemistry of polyoxometallates. actual variation on an old theme with interdisciplinary references. *Angew Chem, Int Ed Engl* 30:34–48
- M.T. Pope and A. Müller, *Polyoxometalates: From Platonic Solids to Anti-Retroviral Activity* (Springer, 1994)
- T. Yamase and M.T. Pope, *Polyoxometalate Chemistry for Nano-Composite Design* (Springer, 2002).
- Sokolov MN, Adonin SA, Peresykina EV, Fedin VP (2012) A Pt(II) isopolytungstate: synthesis and crystal structure. *Dalton Trans* 41:11978–11979
- Lin Z, Izarova NV, Kondinski A, Xing X, Haider A, Fan L, Vankova N, Heine T, Keita B, Cao J, Hu C, Kortz U (2016) Platinum-containing polyoxometalates: *syn*- and *anti*-[Pt^{II}₂(α -PW₁₁O₃₉)₂]¹⁰⁻ and formation of the metal-metal-bonded di-Pt^{III} derivatives. *Chem Eur J* 22:5514–5519
- Kato M, Kato CN (2011) A Keggin-type polyoxotungstate-coordinated diplatinum(II) complex: synthesis, characterization, and stability of the cis-platinum(II) moieties in dimethylsulfoxide and water. *Inorg Chem Commun* 14:982–985
- Kato CN, Morii Y, Hattori S, Nakayama R, Makino Y, Uno H (2012) Diplatinum(II)-coordinated polyoxotungstate: synthesis, molecular structure, and photocatalytic performance for hydrogen evolution from water under visible-light irradiation. *Dalton Trans* 41:10021–10027
- Hattori S, Ihara Y, Kato CN (2015) A novel photocatalytic system constructed using eosin Y, titanium dioxide, and Keggin-type platinum(II)- and aluminum(III)-coordinated polyoxotungstates for hydrogen production from water under visible light irradiation. *Catal Lett* 145:1703–1709
- Kato CN, Suzuki S, Ihara Y, Aono K, Yamashita R, Kikuchi K, Okamoto T, Uno H (2016) Hydrogen evolution from water under visible-light irradiation using Keggin-type platinum(II)-coordinated phospho-, silico-, and germanotungstates as co-catalysts. *Modern Res Catal* 5:103–129
- Kato CN, Suzuki S, Mizuno T, Ihara Y, Kurihara A, Nagatani S (2019) Syntheses and characterization of α -Keggin- and α_2 -Dawson-type diplatinum(II)-coordinated polyoxotungstates: effects of skeletal structure, internal element, and nitrogen-containing ligand coordinated to the platinum center for hydrogen production from water under light irradiation. *Catal Today* 332:2–10
- Kato CN, Aono K, Kurihara A, Kubota T, Kasai R, Suzuki K (2020) Thermal treatment of a Keggin-type diplatinum(II)-coordinated polyoxotungstate: formation of hydrophilic colloidal particles and photocatalytic hydrogen production. *Eur J Inorg Chem* 2020:3917–3924
- Rosenheim A, Jaenicke J (1917) Iso- and heteropolyacids. XV. heteropoly tungstates and some heteropoly molybdates. *Z Anorg Allg Chem* 101:235–275
- Tézé A, Hervé G (1990) α -, β -, and γ -Dodecatungstosilic acids: isomers and related lacunary compounds. *Inorg Synth* 27:85–96
- Tézé A, Hervé G (1977) Formation and isomerization of undeca- and dodecatungstosilicate and -germanate isomers. *J Inorg Nucl Chem* 39:999–1002
- Ivannikova NV, Solodovnikov SF (1995) Refinement of the phase diagram of the Cs₂WO₄-WO₃ system. *Russ J Inorg Chem* 40:1660–1665
- Narasimharao K, Brown DR, Lee AF, Newman AD, Siril PF, Tavener SJ, Wilson K (2007) Structure-activity relations in Cs-doped heteropolyacid catalysts for biodiesel production. *J Catal* 248:226–234
- El-Ghannam A, Chandrasekaran S, Sultana F (2021) Synthesis and characterization of a novel nonowire-reinforced SiC thermal material. *J Solid State Chem* 297:122055
- Liu X, Li Y, Peng S, Lu G, Li S (2012) Photocatalytic hydrogen evolution under visible light irradiation by the polyoxometalate α -[AlSiW₁₁(H₂O)₃₉]⁵⁻-eosin Y system. *Int J Hydrogen Energy* 37:12150–12157
- Liu X, Li Y, Peng S, Lu G (2013) Li S (2013) Photosensitization of SiW₁₁O₃₉⁸⁻-modified TiO₂ by eosin Y for stable visible-light H₂ generation. *Int J Hydrogen Energy* 38:11709–11719
- Li Y, Xie C, Peng S, Lu G, Li S (2008) Eosin Y-sensitized nitrogen-doped TiO₂ for efficient visible light photocatalytic hydrogen evolution. *J Mol Catal A Chem* 282:117–123
- Liu X, Li Y, Peng S, Lu G, Li S (2013) Modification of TiO₂ with sulfate and phosphate for enhanced eosin Y-sensitized hydrogen evolution under visible light illumination. *Photochem Photobiol Sci* 12:1903–1910
- Li Y, Guo M, Peng S, Lu G, Li S (2009) Formation of multilayer-Eosin Y-sensitized TiO₂ via Fe³⁺ coupling for efficient visible-light photocatalytic hydrogen evolution. *Int J Hydrogen Energy* 34:5629–5636
- Dessal C, Martínez L, Maheu C, Len T, Morfin F, Rousset JL, Puzenat E, Afanasiev P, Aouine M, Soler L, Llorca J, Piccolo L (2019) Influence of Pt particle size and reaction phase on the photocatalytic performances of ultradispersed Pt/TiO₂ catalysts for hydrogen evolution. *J Catal* 375:155–163

Publisher's Note Springer Nature remains neutral with regard to jurisdictional claims in published maps and institutional affiliations.